Available online at www.sciencedirect.com
ScienceDirect
Journal of the European Ceramic Society 29 (2009) 565–570
www.elsevier.com/locate/jeurceramsoc

Photocatalytic activity of oxide coatings on fired clay substrates

M. Fassier [a,b], N. Chouard [a], C.S. Peyratout [a,*], D.S. Smith [a], H. Riegler [c], D.G. Kurth [c], C. Ducroquetz [b], M.A. Bruneaux [b]

[a] *Groupe d'Etude des Matériaux Hétérogènes, Ecole Nationale Supérieure de Céramique Industrielle, 47-73 avenue Albert Thomas, 87065 Limoges Cedex, France*
[b] *Centre Technique de Matériaux Naturels de Construction, 17 rue Letellier, 75015 Paris, France*
[c] *Max Planck Institute of Colloids and Interfaces, Am Mühlenberg 1, D-14476 Potsdam-Golm, Germany*

Received 18 March 2008; received in revised form 15 July 2008; accepted 16 July 2008
Available online 7 September 2008

Abstract

The coating of fired clay substrates with various metal oxides, such as anatase, rutile, zinc oxide and tin oxide was achieved using a simple spraying technique followed by a thermal treatment. The photocatalytic activity of the layer was characterized through measurement of the absorption spectrum, in the range 400–800 nm, of methylene blue deposited on top of the coating. Results show that the presence of anatase enhances the degradation of methylene blue when it is exposed to ultraviolet light. Thermal treatment at 1050 °C transforms anatase crystals into thermodynamically stable rutile. This results in a decrease of the photocatalytic activity, which can be explained by increase of the grain size and by a difference in the crystal structure. Measurements of the photocatalytic activity of ZnO and SnO_2 show that these two oxides also exhibit photocatalytic properties. In particular, ZnO is a promising alternative material to anatase.

Keywords: TiO_2; Spectroscopy; Films; Surfaces; Fired clay products

1. Introduction

Besides aesthetic considerations, the development and proliferation of micro-organisms on clay products can cause mechanical and chemical damage to the material. Titanium oxide and zinc oxide are well known as active catalysts for degradation of dyes.[1–5] Indeed, the metastable polymorph of TiO_2, anatase, is currently the most commonly used catalyst for the photodegradation of organic pollutants.[6]

Photocatalysis requires the exposure of a semiconductor, like anatase to UV light. When the energy of the photon is equal or greater than the energy of the band gap of TiO_2, the electrons of the valence band are excited into the conduction band (e_{CB}^-), leaving a hole or an electron vacancy in the valence band (h_{VB}^+).

$$TiO_2 + h\nu \rightarrow TiO_2(e_{CB}^- + h_{VB}^+) \quad (1)$$

If charge separation is maintained, the electrons and holes can migrate to the catalyst surface where they participate in redox reactions with adsorbed species.[7] In particular, h_{VB}^+ may combine with H_2O or OH^- to produce the hydroxyl radical.[8]

$$H_2O_{(ads)} + h_{VB}^+ \rightarrow HO_{(ads)}^\bullet + H_{(ads)}^+ \quad (2)$$

and e_{CB}^- can be picked up by oxygen to generate superoxide radicals.[9,10] These superoxide radicals can in turn generate hydroperoxide and hydrogen peroxide, decomposed at the semiconductor surface into hydroxyl radicals, as described in the following reaction steps:

$$O_{2(ads)} + e_{CB}^- \rightarrow O_{2(ads)}^{\bullet -} \quad (3)$$

$$O_{2(ads)}^{\bullet -} + H_{(ads)}^+ \rightarrow HO_{2(ads)}^\bullet \quad (4)$$

$$HO_{2(ads)}^\bullet + e_{CB}^- + H_{(ads)}^+ \rightarrow H_2O_{2(ads)} \rightarrow 2HO_{(ads)}^\bullet \quad (5)$$

These very reactive radicals can oxidize the adsorbed organic pollutants to achieve complete decomposition.

The efficiency of titanium oxide is influenced by several factors such as the crystallinity of the anatase phase,[6,11] the specific surface area related to particle size and shape[12] and the method of preparation.[13,14]

* Corresponding author. Tel.: +33 5 55 45 22 32; fax: +33 5 55 79 09 98.
E-mail address: claire.peyratout@unilim.fr (C.S. Peyratout).

0955-2219/$ – see front matter © 2008 Elsevier Ltd. All rights reserved.
doi:10.1016/j.jeurceramsoc.2008.07.022

The aim of this paper is to study the influence of the nature of the oxides on the photocatalytic activity of the fired clay substrate coatings. Micro-organisms were mimicked with the standard dye methylene blue as a substitute molecule to evaluate photocatalytic efficiency: the decomposition of methylene blue is accompanied by its discolouration from a vivid blue to a colourless hue.

2. Experimental

2.1. Materials and preparation of photocatalysts

Titanium(IV) oxide (anatase from Prolabo VWR, Fontenay-sous-Bois) was chosen for the preparation of a photocatalytic layer for the fired clay substrate. This product consists of 93% anatase and 7% rutile with a specific surface area of 10.7 $m^2\ g^{-1}$ (measured with the BET method) and a primary particle size of 150 nm.

Titanium(IV) oxide TiO_2 (rutile) was obtained from Prolabo VWR, Fontenay-sous-Bois, France. It is composed of 88% rutile and 12% anatase with a specific surface area (BET) of 1.39 $m^2\ g^{-1}$ and a primary particle size of 1.05 μm. Zinc oxide (Ceradel, Limoges, France), crystallizes as zincite, has a specific surface area (BET) of 3.3 $m^2\ g^{-1}$ and a primary particle size of 336 nm. Tin oxide, supplied by Ceradel, Limoges, France, crystallizes as cassiterite and exhibits a specific BET-surface area of 5.4 $m^2\ g^{-1}$ and a primary particle size of 165 nm. An alternative approach, which avoids the necessity of thermal treatment, was based on depositing anatase onto an intermediate layer of alumina cement (SECAR 71) prepared by the company Cimentys (Limoges). This intermediate layer consists of more than 70% of alumina with a specific surface area of 0.74 $m^2\ g^{-1}$ (measured with the BET method).

Methylene blue was obtained from Kuhlmann (Bordeaux, France). It was used without any further purification. Throughout this study, distilled water and denatured ethanol (97%, Elvetec, Genas, France) were used.

2.2. Sample preparation

Substrates in the form of square-shaped slabs were cut, with dimensions 4 cm × 4 cm × 1 cm, out of a commercial fired clay product. Two types of fired clay substrate named R and S for rough and smooth, respectively were used. The R substrates were coated as received while S substrates were mechanically polished prior to coating. In both cases, the apparent open porosity was evaluated at 19.4%.

Two techniques to achieve adherence of the anatase particles onto the substrates were tested:

- In a first set of experiments, a heat treatment after spraying of the anatase powder was used. 10 g of the anatase powder was dispersed in 90 g of distilled water. The suspension was then mixed for 15 min in a tubular agitator before being sprayed onto the fired clay substrate. The sample is subsequently fired at 850 °C for 2 h (temperature ramp: 10 °C/min).

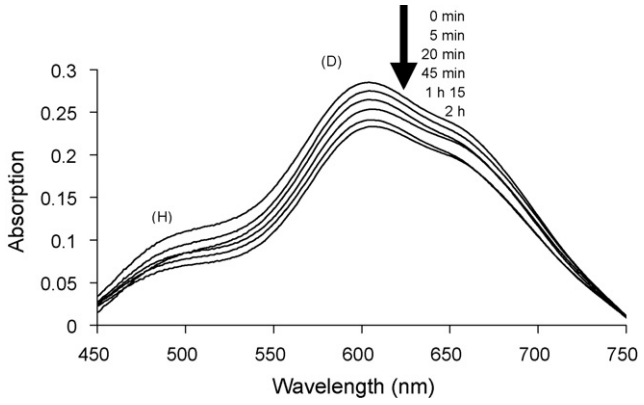

Fig. 1. Influence of the irradiation time on the absorption spectra of methylene blue adsorbed on fired clay substrates.

- In a second approach to achieve adherence, first, alumina-based cement was mixed in a liquid additive for 3 min before being sprayed onto the substrate. Then, the anatase suspension was sprayed onto the first layer to form the photocatalytic coating. To finish, samples, covered with these two layers, were dried for 24 h in a humid atmosphere.

The other oxides (rutile, zinc oxide and tin oxide) were prepared in a similar manner to the anatase coating fixed by heat treatment. The concentration of oxide in the suspension and the firing conditions were identical.

For experiments involving exposure to UV light, the coated samples were soaked in a 10^{-5} mol l^{-1} methylene blue solution for 30 min and then dried for 12 h in a dark room.

2.3. Analysis

Methylene blue degradation was monitored using a UV–vis Spectrophotometer (ElmerPerkin Lambda 40). Since the samples are solid and opaque, the absorption measurements are made with an integrating sphere, which collects the reflected beam from the sample. Samples were exposed to UV light (λ = 366 nm) for 2 h, and measurements were recorded at regular time intervals. Fig. 1 shows the methylene blue adsorption spectra for a smooth substrate (S) following different irradiation times. Three peaks, centered on 555, 600 and 660 nm can be identified and are attributed to the presence of H-aggregates, dimers and monomers, respectively in methylene blue. The relation between absorption of light, A, and concentration of the absorbing species, C, is described by the Beer–Lambert law.

$$A = \varepsilon b C \tag{6}$$

where b is the optical pathlength in cm and ε is the extinction coefficient in $cm^{-1}\ l\ mol^{-1}$. The extinction coefficient for each species is assumed to be the same.[15–17] The ratio of concentration of methylene blue, at a time t, C_t to the concentration at time zero, C_0, is given by the ratio of the measured absorption A_t at time t to the initial absorption A_0. Though there is an interdependent relationship between the three species, it has been found convenient to choose the strong dimer peak to represent the concentration of methylene blue. In fact, a slight red shift can

be detected in the 600 nm dimer peak explained by the conversion of dimers into monomers. The absorption ratio A_t/A_0 of this peak has therefore been studied as a function of irradiation time. XRD experiments were carried out using a diffractometer with the Debye–Scherrer geometry, based on a sealed tube operating at 37.5 kV/28 mA, a curved quartz monochromator (Cu $K\alpha_1$ radiation) and a curved position sensitive detector (Inel CPS 120).

Topographic measurements of the samples were made at room temperature with a Nanoscope IIIa scanning probe microscope (Digital Instrument). The microscope was operated in the tapping scanning mode. The scanning probes were batch fabricated Si cantilevers with CN–W alloy coated tips. Details of the tip are: size, 160 μm × 45 μm × 4.6 μm; radius of curvature, 10 nm; spring constant, 42 N/m; resonance frequency, 285 kHz.

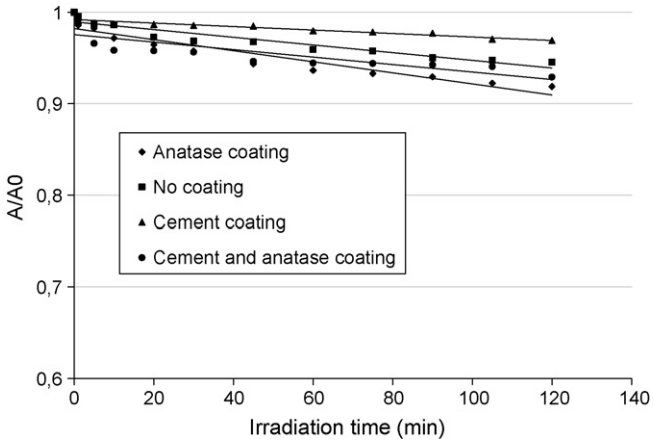

Fig. 2. Normalized absorption of light at 600 nm by methylene blue as a function of UV exposure time for different coatings on smooth fired clay substrates.

3. Results and discussion

3.1. Effect of the irradiation time

If the degradation of methylene blue obeys first order kinetics, then the concentration of methylene blue can be described by

$$C_t = C_0 \exp(-kt) \quad (7)$$

where k represents the apparent rate constant. For short times, the dependence of the normalized absorption A_t/A_0 on time can be modelled as a straight line. The slope gives a direct measure of the degradation rate constant.[18] The absorption spectra for methylene blue were found to be of similar form for both smooth and rough fired clay substrates. The same general trend of degradation behavior with UV exposure time was also obtained on the two types of substrate. However, the amount of methylene blue adsorbed on a smooth substrate is twice as much as the amount adsorbed on a rough substrate. We deduce that both the chemical nature of the substrate surface as well as its roughness have an influence in the affinity of the substrate for methylene blue.

Experiments were carried out with different coatings composed of alumina-based cement, anatase and a mixture of anatase and cement. The concentration of anatase in the coatings was kept constant at 10% in mass. The concentration in methylene blue was fixed at 10^{-5} mol l^{-1} and smooth substrates were used. Fig. 2 and Table 1 show that the decomposition rate of dimers in methylene blue with the UV light irradiation time is highest with an anatase coating. In the presence of alumina cement, the decomposition rate of methylene blue is lower than that observed for blank samples, implying that alumina cement inhibits the decomposition of methylene blue. Indeed, a mixture of cement and anatase as a coating is less effective than no coating at all. Moreover, the plot of A/A_0 as a function of the irradiation time is no longer linear ($R^2 = 50$ for a rough sample with cement). It is then difficult to assign a reaction order. Several reasons can explain the discrepancy between the experimental results and the expected behavior. Aging of the catalyst surface and pH changes, especially on cement surfaces could explain these results. Somewhat similar behavior with unknown reaction order, although at longer exposure times, has been observed during the removal of organic contaminants in paper pulp by TiO_2 photocatalyzed oxidation.[19] Results obtained on rough substrates follow the same trends and are also presented in Table 1.

To conclude, anatase powder deposited on the surface of fired clay substrates with a heat treatment enhances the photocatalytic decomposition of a model system, the dye methylene blue. However, the presence of an alumina-based cement matrix inhibits methylene blue decomposition.

3.2. Influence of firing temperature

To evaluate the impact of the thermal treatment on the photocatalytic activity of anatase, spectrophotometric measurements were carried out on a series of smooth samples and a series of rough samples covered by anatase layers deposited from

Table 1
Rate of decomposition of dimers of methylene blue and correlation coefficients for different coatings on smooth (S) and rough (R) substrates

	Coating			
	No coating (reference)	Anatase	Alumina-based cement	Anatase and alumina-based cement
Smooth substrates (S)				
Slope ($\times 10^{-5}$)	−42	−60.4	−19.1	−22.8
R^2 (%)	90	90	88	91
Rough substrates (R)				
Slope($\times 10^{-5}$)	−65.1	−108.5	−13.8	−22.8
R^2 (%)	99	94	50	91

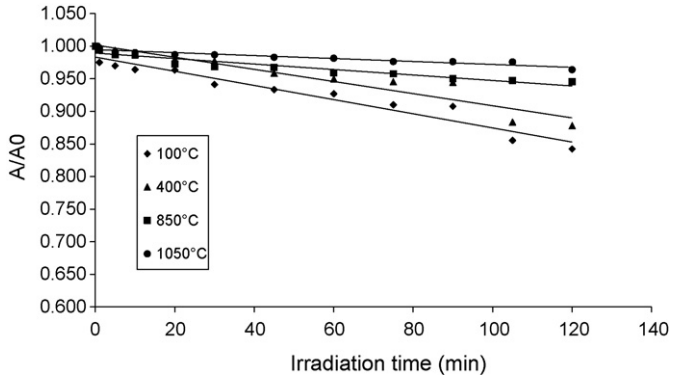

Fig. 3. Evolution of the rate of degradation of methylene blue dimers adsorbed on (S) fired clay substrates with the firing temperature.

Table 2
Rate of decomposition of dimers of methylene blue for different firing temperatures on smooth substrates

	Temperature of firing (°C)			
	100	400	850	1050
Slope ($\times 10^{-5}$)	−109	−93	−42	−22.8
R^2 (%)	94	92	90	91

an aqueous suspension. Both types of sample were subjected to thermal treatments at 100, 850, 950 or 1050 °C. Fig. 3 and Table 2 show that the rate of decomposition of dimers of methylene blue is highest when the thermal treatment temperature is low (100 °C). For a thermal treatment temperature of 850 °C, the decomposition of dimers of methylene blue has slowed down to a rate close to or slightly higher than the value observed for a sample without coating.

XRD patterns were then recorded for the coatings following thermal treatment at the different temperature. In comparison with the JCPDS data cards, the diffraction patterns are indexed without difficulty to anatase and rutile. The lattice constants (in Å) calculated from the diffraction peaks are $a = 3.78$, $c = 9.51$ for anatase and $a = 4.58$, $c = 2.95$ for rutile, respectively. These are in good agreement with those of anatase and rutile single crystal ($a = 3.7842$, $c = 9.5146$ for an anatase single crystal and $a = 4.5845$, $c = 2.953$ for a rutile single crystal). In addition, no peaks from other impurities were detected in the patterns. An increase in the diffraction peak intensity was observed upon increasing the heating temperature, which means that the crystallinity of the TiO_2 powder was enhanced at higher temperature. The X-ray diffraction measurements were also used to study coherent domain size evolution in the anatase/rutile powders in relation to the thermal treatment. The full width at half maximum height (FWMH) of a peak in the diffraction pattern is related to the coherent domain size: D (and thus the crystallite size) using the simplified Scherrer relation:

$$D = \frac{0.9\lambda}{\Delta(2\theta)\ \cos\theta} \tag{8}$$

where λ is the wavelength of the Cu Kα_1 radiation. $\lambda = 1.5408$ Å; θ is the angle of diffraction in radian; $\Delta(2\theta)$ is the FWMH in radian.

The FWMH for the three most intense peaks characteristic of anatase or rutile show that the coherent domain size increases from 41 nm for a thermal treatment at 100 °C to 57 nm for a treatment at 1050 °C (see Fig. 4). Scanning probe measurements on titanium oxide particles synthesized with a sol–gel method[20] and deposited on silicon wafers confirm this trend. In this particular case, the average grain size increases from 22 nm at 500 °C to 79 nm at 1000 °C. In parallel, BET measurements indicated that the specific surface area of anatase powder decreased from 11.7 $m^2\ g^{-1}$ for a thermal treatment at 100 °C to 2.1 $m^2\ g^{-1}$ for a thermal treatment at 1050 °C. Thus, as the thermal treatment temperature increases, the specific surface area of the catalyst decreases which can be correlated to the decrease in photocatalytic activity, shown in Fig. 3.

The other important factor is the proportion of anatase to rutile in the powder. According to the X-ray data, the proportion of anatase is maintained at its original level of 93% for thermal treatment up to 840 °C. Above this thermal treatment temperature, the anatase crystals transform into rutile. Complete

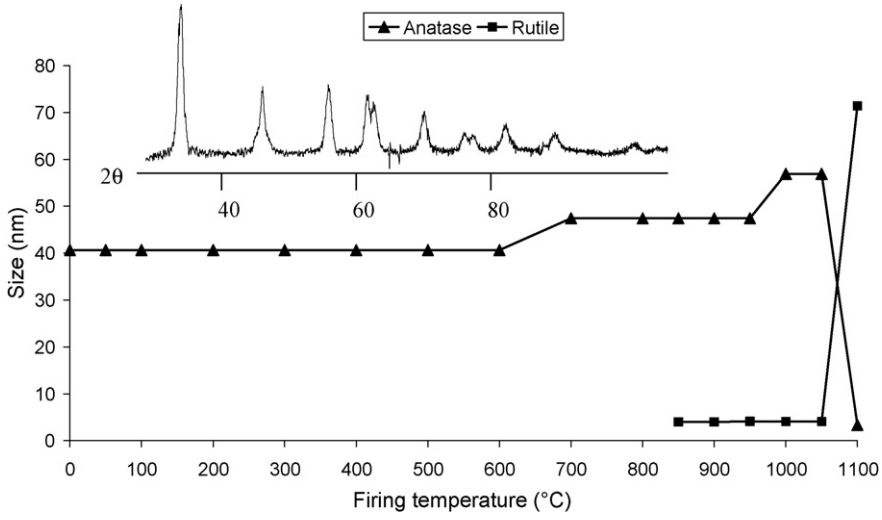

Fig. 4. Evolution of the coherent domain size as a function of the firing temperature of the anatase coatings. Inset: X-ray diagram of anatase crystals at 400 °C.

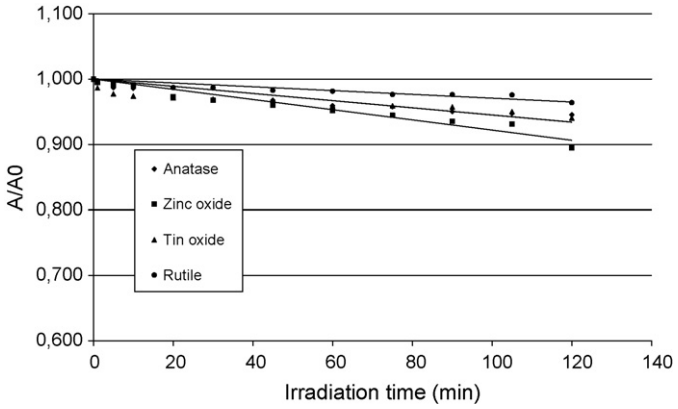

Fig. 5. Evolution of rate of degradation of methylene blue dimers adsorbed on (S) fired clay substrates with the nature of the oxide used.

(100%) transformation is achieved for temperatures greater than 1050 °C. Correspondingly the decomposition rate of methylene blue is much slower, which can be attributed to smaller specific surface area of the powder and also to the lower photocatalytic activity of rutile.[21,22]

To summarize, increase in firing temperature causes an increase of the average particle size and an increase of the proportion of the rutile in the titanium dioxide coating. Both factors decrease the photocatalytic behavior of the deposited layer.

3.3. Influence of the nature of the oxides

Finally, we investigated if other wide band gap semiconducting oxides could have a photocatalytic activity similar to anatase. Samples were first sprayed by an aqueous suspension of either anatase, rutile, zinc oxide or tin oxide. Samples were then fired and the probe dye was deposited as described previously. Spectrophotometric measurements following the variations of absorption of methylene blue as a function of time for the different metal oxides are presented in Fig. 5. This suggests that the degradation of methylene blue deposited on a fired clay product covered with a predominantly rutile-based coating is slower than with an anatase layer. Since the average particle size of the two powders are so different, it is difficult to conclude which parameter between grain size and oxide nature is controlling the photocatalytic effect. However, other workers have already demonstrated the difference in photocatalytic activity between anatase and rutile.[21,22] This behavior has been attributed to the crystallographic differences between the two polymorphs and the influence of defects.[23] Planes at the surface of rutile probably present different characteristics from the photocatalytic active ones formed by the oxygen atoms on anatase crystals.[21]

Surprisingly, coarse (340 nm) zinc oxide crystals are better photocatalysts than finer anatase ones (150 nm, see Table 3). This was explained by the greater quantum efficiency of ZnO compared to TiO_2 and other oxides.[24] Reduced photocatalytic activity in tin oxide can be explained because of the wide band gap (3.9 eV compared with 3.2 eV for anatase and ZnO). The light energy in this band at shorter wavelengths is insufficient to generate many electron-hole pairs.[24]

Table 3
Rate of decomposition of dimers of methylene blue for different oxides on smooth substrates

	Oxide			
	TiO_2 anatase	TiO_2 rutile	ZnO	SnO_2
Slope ($\times 10^{-5}$)	−42	−22.8	−72.4	−34.8
R^2 (%)	99	91	98	87
Grain size (nm)	150	1050	336	165
Specific area ($m^2\ g^{-1}$)	10.7	1.39	3.3	5.4

4. Conclusions

We have described techniques to deposit a coating of anatase and other semiconductors such as ZnO, SnO_2 or rutile on fired clay products. The coating is fixed by thermal treatment or by using a sublayer of alumina-based cement. According to spectrophotometric measurements, TiO_2, as metastable anatase, efficiently catalyses the decomposition of dye like methylene blue in the presence of light and oxygen on fired clay substrates. In comparison, alumina-based cement coating decomposes methylene blue even more slowly than a fired clay product without any coating. The thermal treatment temperature of the anatase coating is a significant parameter which influences the photocatalytic activity of the coating due to changes in the specific surface area and anatase/rutile ratio of the powder. Finally, the photocatalytic activity of several different semiconductor oxide coatings has been compared. Significantly, rutile is a poor photocatalyst whereas zinc oxide provides a good alternative to titanium oxide.

Acknowledgements

The authors would like to thank Prof. Helmuth Moehwald, director of the Interface Department, for logistic support of Nolwenn Chouard's internship and Mrs. Anneliese Heilig and Dr. Radu-Cristian Mutihac for their help with the AFM measurements at the MPI-KG in Potsdam.

References

1. Fujishima, A., Hashimoto, K. and Watanabe, T., *TiO_2 Photocatalysis Fundamentals and Applications*. Bkc Inc., Tokyo, 1999.
2. Neppolian, B., Choi, H. C., Sakthivel, S., Arabindoo, B. and Murugesan, V., Solar light induced and TiO_2 assisted degradation of textile dye reactive blue 4. *Chemosphere*, 2002, **46**, 1173–1181.
3. Serpone, N. and Pelizetti, E., *Photocatalysis: Fundamentals and Applications*. Wiley, New York, 1989.
4. Konstantinou, I. K. and Albanis, T. A., Photocatalytic transformation of pesticides in aqueous titanium dioxide suspensions using artificial and solar light: intermediates and degradation pathways. *Applied Catalysis B: Environmental*, 2003, **42**, 319–335.
5. Vulliet, E., Emmelin, C., Chovelon, J. M., Guillard, C. and Herrmann, J. M., Photocatalytic degradation of sulfonylurea herbicides in aqueous TiO_2. *Applied Catalysis B: Environmental*, 2002, **38**, 127–137.
6. Fox, M. A. and Dulay, M. T., Heterogeneous photocatalysis. *Chemical Reviews*, 1993, **93**, 341–357.
7. Hoffmann, M. R., Martin, S. T., Choi, W. and Bahnemann, D. W., Environmental applications of semiconductor photocatalysis. *Chemical Reviews*, 1995, **95**, 69–96.

8. Peral, J., Domenech, X. and Ollis, D. F., Heterogeneous photocatalysis for purification, decontamination and deodorization of air. *Journal of Chemical Technology and Biotechnology*, 1997, **70**, 117–140.
9. Turchi, C. S., Ollis, D. F. and Matthews, R. W., Photocatalytic reactor design: an example of mass-transfer limitations with an immobilized catalyst. *Journal of Physical Chemistry*, 1998, **92**, 6852–6853.
10. Matthews, R. W. and McEvoy, S. R., Destruction of phenol in water with sun, sand, and photocatalysis. *Solar Energy*, 1992, **49**, 507–513.
11. Ohtani, B., Osaki, H., Nishimoto, S. I. and Kagiya, T., A novel photocatalytic process of amine *N*-alkylation by platinized semiconductor particles suspended in alcohols. *Journal of the American Chemical Society*, 1986, **108**(2), 308–310.
12. Zhang, H., Wang, C. C., Zakaria, R. and Ying, J. Y., Enhanced adsorption of molecules on surfaces of nanocrystalline particles. *Journal of Physical Chemistry B*, 1999, **103**, 4656–4662.
13. Madhusudan Reddy, K., Gopal Reddy, C. V. and Manorama, S. V., Preparation, characterization, and spectral studies on nanocrystalline anatase TiO_2. *Journal of Solid State Chemistry*, 2001, **158**, 180–186.
14. Wang, C. C. and Ying, J. Y., Sol–gel synthesis and hydrothermal processing of anatase and rutile titania nanocrystals. *Chemistry of Materials*, 1999, **11**, 3113–3120.
15. Spencer, W. and Sutter, J. R., Kinetic study of the monomer–dimer equilibrium of methylene blue in aqueous solution. *Journal of Physical Chemistry*, 1979, **83**, 1573–1576.
16. Kobayashi, H., Takahashi, M. and Kotani, M., Spontaneous formation of an ordered structure during dip-coating of methylene blue on fused quartz. *Chemical Physics Letters*, 2001, **349**, 376–382.
17. Ohline, S. M., Lee, S., Willams, S. and Chang, C., Quantification of methylene blue aggregation on a fused silica surface and resolution of individual absorbance spectra. *Chemical Physics Letters*, 2001, **346**, 9–15.
18. Senthilkumar, K., Prokodi, R. and Vidyalakshmi, R., Photodegradation of a textile dye catalyzed by sol–gel derived nanocrystalline TiO_2 via ultrasonic irradiation. *Journal of Photochemistry and Photobiology A: Chemistry*, 2005, **170**, 225–232.
19. Perez, M., Torrades, F., Garcia-Hortal, J. A., Domenech, X. and Peral, J., Removal of organic contaminants in paper pulp treatment effluents by TiO_2 photocatalyzed oxidation. *Journal of Photochemistry and Photobiology A*, 1997, **109**, 281–286.
20. Jensen, M. J. and Fuierer, P. A., Low temperature preparation of nanocrystalline anatase films through a sol-gel method. *Journal of Sol–Gel Science and Technology*, 2006, **39**, 229–233.
21. Ding, Z., Lu, G. Q. and Greenfield, P. F., Role of the crystallite phase of TiO_2 in heterogeneous photocatalysis for phenol oxidation in water. *Journal of Physical Chemistry B*, 2000, **104**, 4815–4820.
22. Diebold, U., Ruzycki, N., Herman, G. S. and Selloni, A., One step towards bridging the materials gap: surface studies of TiO_2 anatase. *Catalysis Today*, 2003, **85**, 93–100.
23. Ganduglia-Pirovano, M., Hofmann, A. and Sauer, J., Oxygen vacancies in transition metal and rare earth oxides: current state of understanding and remaining challenges. *Surface Science Reports*, 2007, **62**, 219–270.
24. Kansal, S. K., Singh, M. and Suc, D., Studies on photodegradation of two commercial dyes in aqueous phase using different photocatalysts. *Journal of Hazardous Materials*, 2007, **141**, 581–590.